Z. Phys. C – Particles and Fields 42, 189–197 (1989)

Zeitschrift für Physik C Particles and Fields

Pion, kaon and proton cross sections in $e^+ e^-$ annihilation at 34 GeV and 44 GeV c.m. energy

TASSO Collaboration

W. Braunschweig, R. Gerhards, F.J. Kirschfink, H.-U. Martyn
I. Physikalisches Institut der RWTH, Aachen, Federal Republic of Germany[a]

B. Bock[1], H.M. Fischer, H. Hartmann, J. Hartmann, E. Hilger, A. Jocksch, R. Wedemeyer
Physikalisches Institut der Universität, Bonn, Federal Republic of Germany[a]

B. Foster, A.J. Martin, A.J. Sephton
H.H. Wills Physics Laboratory, University of Bristol, Bristol, UK[b]

F. Barreiro[14], E. Bernardi[2], J. Chwastowski[3], A. Eskreys[4], K. Gather, K. Genser[5], H. Hultschig, P. Joos, H. Kowalski, A. Ladage, B. Löhr, D. Lüke, P. Mättig[6], D. Notz, J.M. Pawlak[7], K.-U. Pösnecker, E. Ros, D. Trines, R. Walczak[5], G. Wolf
Deutsches Elektronen-Synchrotron DESY, Hamburg, Federal Republic of Germany

H. Kolanoski
Institut für Physik, Universität, Dortmund, Federal Republic of Germany[a]

W. Gerhardt, T. Kracht[8], H.L. Krasemann[16], J. Krüger, E. Lohrmann, G. Poelz, P. Rehders, G. Tysarczyk[17], C. Winand[18], W. Zeuner
II. Institut für Experimentalphysik der Universität, Hamburg, Federal Republic of Germany[a]

D.M. Binnie, J. Hassard, J. Shulman, D. Su[15]
Department of Physics, Imperial College, London, UK[b]

A. Leites, J. del Peso
Universidad Autonoma de Madrid, Madrid, Spain[c]

C. Balkwill, M.G. Bowler, P.N. Burrows[15], R. Cashmore, G.P. Heath, P.N. Ratoff, I.M. Silvester, I.R. Tomalin[19], M.E. Veitch
Department of Nuclear Physics, Oxford University, Oxford, UK[b]

G.E. Forden[9], J.C. Hart, D.H. Saxon
Rutherford Appleton Laboratory, Chilton, Didcot, UK[b]

S. Brandt, M. Holder, L. Labarga[10]
Fachbereich Physik der Universität-Gesamthochschule, Siegen, Federal Republic of Germany[a]

Y. Eisenberg, U. Karshon, G. Mikenberg, A. Montag, D. Revel, E. Ronat, A. Shapira, N. Wainer, G. Yekutieli
Weizmann Institute, Rehovot, Israel[d]

A. Caldwell[11], D. Muller, S. Ritz[11], D. Strom[12], M. Takashima, E. Wicklund[13], Sau Lan Wu, G. Zobernig
Department of Physics, University of Wisconsin, Madison, Wis., USA[e]

Received 22 November 1988

[1] Now at Krupp Atlas Elektr. GmbH, Bremen, FRG
[2] Now at Robert Bosch GmbH, Schwieberdingen, FRG
[3] On leave from Inst. of Nuclear Physics, Cracow, Poland
[4] Now at Inst. of Nuclear Physics, Cracow, Poland
[5] Now at Warsaw University, Poland; partially supported by grant CPBP 01.06
[6] Now at IPP Canada, Carleton University, Ottawa, Canada
[7] On leave from Warsaw University, Poland; partially supported by grant CPBP 01.06
[8] Now at Hasylab, DESY, Hamburg, FRG
[9] Now at SUNY Stony Brook, Stony Brook, NY, USA
[10] Now at SLAC, Stanford, CA, USA
[11] Now at Columbia University, NY, USA
[12] Now at University of Chicago, Chicago, IL, USA
[13] Now at California Inst. of Technology, Pasadena, CA, USA
[14] Alexander von Humboldt Fellow, on leave of absence from Universidad Autonoma de Madrid, Spain
[15] Now at Rutherford Appleton Laboratory, Chilton, Didcot, UK
[16] Now at GKSS, Geesthacht, FRG
[17] Now at Heidelberg University, FRG
[18] Now at SCS, Hamburg, FRG
[19] Now at Imperial College, London, UK

[a] Supported by Bundesministerium für Forschung und Technologie
[b] Supported by UK Science and Engineering Research Council
[c] Supported by CAICYT
[d] Supported by the Minerva Gesellschaft für Forschung GmbH
[e] Supported by US Dept. of Energy, contract DE-AC02-76ER000881 and by US Nat. Sci. Foundation Grant number INT-8313994 for travel

Abstract. The inclusive production of $\pi^{\pm}$ and $K^{\pm}$ mesons and of protons and antiprotons in e^+e^- annihilations has been measured at 34 GeV and 44 GeV center of mass energy; in addition π^0 mesons have been measured at 44 GeV c.m. energy. Differential cross sections and particle yields are given.

At 34 GeV average multiplicities are:

$\langle n(\pi^{\pm})\rangle = 10.9 \pm 0.5, \quad \langle n(K^{\pm})\rangle = 1.76 \pm 0.20,$

$\langle n(p+\bar{p})\rangle = 0.67 \pm 0.06$

and at 44 GeV:

$\langle n(\pi^{\pm})\rangle = 11.1 \pm 0.5, \quad \langle n(\pi^0)\rangle = 5.4 \pm 1.0.$

1 Introduction

The knowledge of particle composition of the final state in e^+e^- annihilation into hadrons is important for our understanding of the hadronisation process. In the high energy region above the Upsilon resonance first measurements of inclusive spectra of charged pions, kaons and protons [1] and of neutral pions [2] have been carried out by the TASSO Collaboration; subsequently the TASSO group has presented inclusive spectra of charged hadrons identified over the full momentum range at c.m. energies of 14 GeV, 22 GeV and 34 GeV [3], and on π^0 production at 34.6 GeV [4]. Other groups working at SLAC and at DESY have also presented inclusive spectra of $\pi^{\pm}$, $K^{\pm}$, $(p, \bar{p})$ [5] and of neutral pions [6]. In this paper we present inclusive spectra of charged hadrons at 34 GeV c.m. energy with increased statistics and improved treatment of systematic effects, and on charged and neutral pions at 44 GeV c.m. energy, which is the highest energy at which such measurements have been published so far.

2 Experimental procedure

The experiment has been performed with the TASSO detector at the PETRA e^+e^- storage ring. At 34 GeV c.m. energy a total integrated luminosity of 77 pb^{-1} has been used. At an average c.m. energy of 44 GeV the integrated luminosity was 34 pb^{-1}. A description of the detector and of the procedures used to select hadronic events and tracks has been given in our previous publications [3, 7]. The procedure to identify charged hadrons consists of a measurement of the momentum and of the velocity of the particles.

The momentum p is measured with the central drift chamber with an accuracy of

$\sigma_p/p = 0.017 \cdot \sqrt{1+p^2}$ (with p in GeV/c).

For low particle momenta the velocity is measured by time of flight.

Time of flight counters are located behind the central drift chamber at a radial distance of 132 cm from the beam axis (ITOF) and behind the gas Cerenkov counters of the hadron arms [8] at an average distance of 550 cm. The time resolution (rms) of the ITOF counters was 310 ps at the ends of the counters and 480 ps in the middle. Figure 1a and b shows the particle velocity, as measured with the ITOF counters, vs. momentum for the two sets of data at 34 GeV and 44 GeV c.m. energy.

For high momentum particles a system of three threshold Cerenkov counters is used to separate the various hadron species. The Cerenkov counters are filled with aerogel, Freon 114 and CO_2; with threshold momenta for pions of 0.7, 2.7 and 4.8 GeV/c, respectively, and correspondingly higher values for kaons and protons. They are located in two arms (hadron arms) at 90° with respect to be the beam line, subtending a total solid angle of 19% of 4π. In each arm the counters are divided into 16 mechanically separated cells, each one covering 27° in azimuthal and 10° in polar angle.

The determination of the particle fractions has been described in great detail in our previous paper [3], and therefore only points of difference are mentioned here.

The time of flight analysis has been improved by a more detailed calculation of the acceptance and by an improved calibration of the TOF counters [9]. Systematic errors for the particle fractions, as measured by the TOF counters, are largely determined by uncertainties in separating the overlapping velocity distributions of pions, kaons and protons at the larger momenta. In order to determine the particle fractions, we calculated particle masses from the measured momenta and time of flight values, and then fitted the mass distributions to yield the particle fractions. To estimate systematic effects, we also used a weighting method, giving to each track a weight according to its probability of being a pion, kaon or proton, as determined by its time of flight and momentum. For each of the two methods we used four different parametrisations of the assumed mass distributions and weight functions. A comparison of these results allowed a consistency check on the systematic errors.

The systematic errors are 6%–10% of the particle fractions for kaons and protons below 0.8 GeV/c and about 25% in the momentum range 0.8–1.0 GeV/c for kaons and 1.2–2.0 GeV/c for protons where separation by time of flight becomes difficult.

For measurements with the Cerenkov counters, main contributions to the systematic errors come

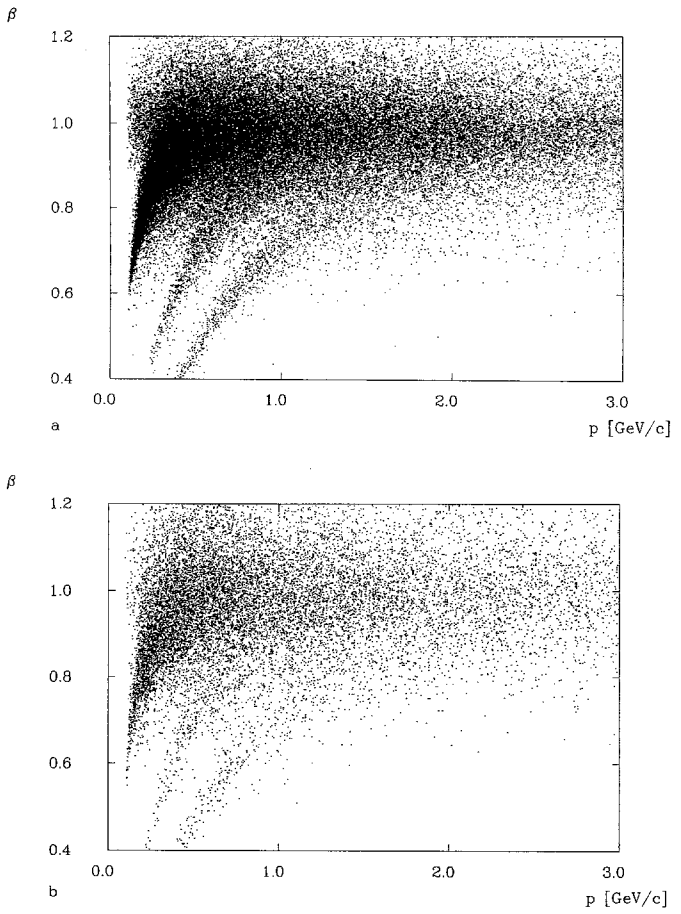

Fig. 1. Particle velocity β vs momentum p for charged particles **a** at 34 GeV, **b** at 44 GeV c.m. energy

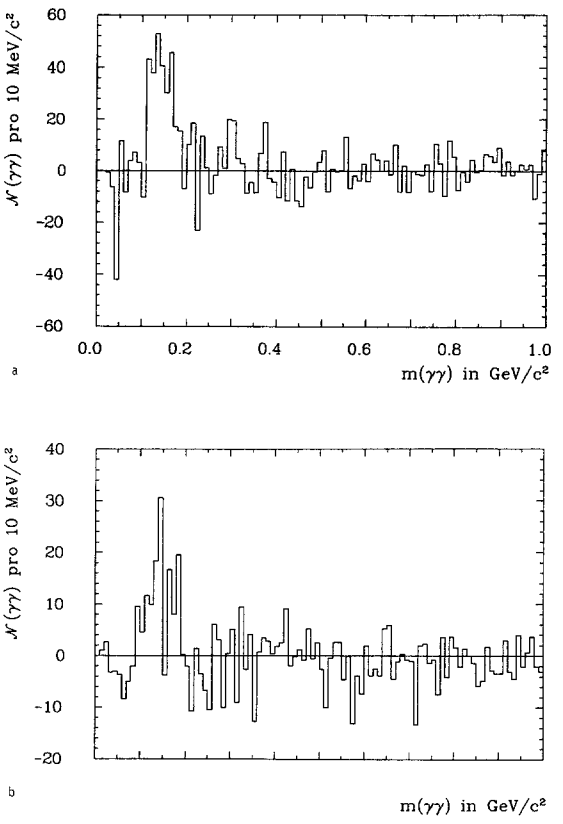

Fig. 2. Invariant $\gamma\gamma$ mass distribution after background subtraction for momenta p of the $\gamma\gamma$ system of **a** $1.0\,\text{GeV/c} < p < 1.5\,\text{GeV/c}$, **b** $4.0\,\text{GeV/c} < p < 6.0\,\text{GeV/c}$

from background and uncertainties in the detection efficiency. Other sources of systematic errors are uncertainties in the corrections for delta electrons, in the muon and electron subtraction and in the correction for absorption. The systematic error for the kaon and proton fractions is 14%, except for the highest momentum interval of 10–17 GeV/c, where it is 23% of the value of the fraction.

For the pion fractions the relative systematic error is 1–2% below 1 GeV/c, where ITOF measurements are possible. At higher momenta the relative systematic error is about 6% between 1.0 and 3.4 GeV/c, about 3% at 4–6 GeV/c and 10% at 10–17 GeV/c.

As a check on the TOF analysis we analysed an independent data sample of $110\,\text{pb}^{-1}$, taken at a c.m. energy of 35 GeV in 1986. We obtained the same results within the errors. However, no data from the Cerenkov counters were available at that energy, and therefore no consistent analysis covering all momenta could be done at that energy, and we chose not to include the 35 GeV data in this paper.

The data have been corrected for a background due to electrons and muons among the charged particles. The particle fractions include the contributions from decay products of particles with an average lifetime smaller than 3.10^{-10} s. For example, the pion fractions include the contribution from $K_s^0 \to \pi^+\pi^-$ decays, and the proton fractions include contributions from Λ decays.

The measurement of the inclusive π^0 spectrum is based on photons detected in the lead-liquid argon barrel calorimeters. The barrel calorimeters are located above and below the magnet coil of the detector. They cover a solid angle of 40% of 4π, extending from $42° \leqq \theta \leqq 138°$ in polar angle and in two sections of azimuthal angle, namely $30° \leqq \Phi \leqq 150°$ and $210 \leqq \Phi \leqq 330°$. The first active layer of the calorimeter is at a radial distance of 178 cm from the interaction point. It is segmented into towers of $7 \times 7\,\text{cm}^2$ area in the front part and $14 \times 14\,\text{cm}^2$ area in the back part. In addition there is a system of orthogonal strips of about 2 cm width, which are used for accurate position and shower profile measurements. Photons are recognized in the calorimeters as clusters of deposited energy. The details of this procedure have been described in our previous paper [4].

The π^0 signal has been extracted by considering the $\gamma\gamma$ invariant mass distribution. The width of the

signal agrees with the results of a Monte Carlo program, which was also used to calculate the background. Details of the background subtraction are given in [10]. Background subtracted mass plots for the lowest and the highest momentum interval are shown in Fig. 2a, b.

Above a π^0 momentum of 6 GeV/c this method of reconstructing the π^0 mass does not work, because the angle between the two photons becomes so small, that the clusters from the two decay photons merge. We have used shower profile measurements at these high energies to distinguish clusters produced by π^0 mesons from those produced by single photons. The details of the method are described in [4]. The details of the method employed to calculate the π^0 cross section from the mass plots are also described in our previous paper [4].

Systematic errors of the π^0 cross section come from uncertainties of the calorimeter acceptance (8%), calorimeter detection efficiency (5%), an overall normalization error of 5%, normalization and correction of the mass plots (10%), and uncertainties in the background subtraction, which varied from bin to bin and were about 10%–15%.

These systematic errors were added in quadrature.

3 Results and Discussion

Figure 3a, b shows the inclusive charged hadron spectra at 34 GeV based on higher statistics than our previous work [11], and at 44 GeV center of mass energy. Defining $x_p = p/p$ (beam), p = particle momentum, we present the data in the form $d\sigma/\sigma_T dx_p$. We took the total hadronic cross section σ_T from our own data, which yielded $R = 3.97$ at 34 GeV and $R = 4.12$ at 44 GeV c.m. energy, with $R = \sigma_T/\sigma_0$ and $\sigma_0 = (4\pi/3) \cdot \alpha^2/s$. All data have been corrected for acceptance losses, initial state bremsstrahlung and smearing due to finite momentum resolution. The inclusive hadron cross section has an overall normalization error of about 6%.

The particle fractions f_π, f_K and f_p at 34 and 44 GeV c.m. energy are shown in Tables 1a, b. These numbers denote the fractions of charged pions, charged kaons and protons plus antiprotons among the produced hadrons, respectively. The charged pion fractions at 34 and 44 GeV c.m. energy are shown in Fig. 4; the charged kaon and proton plus antiproton fractions at 34 GeV c.m. energy are shown in Fig. 5. The errors include systematic and statistical errors added in quadrature.

Inclusive momentum distributions for charged pions, kaons and protons plus antiprotons are then obtained from the inclusive hadron cross sections and

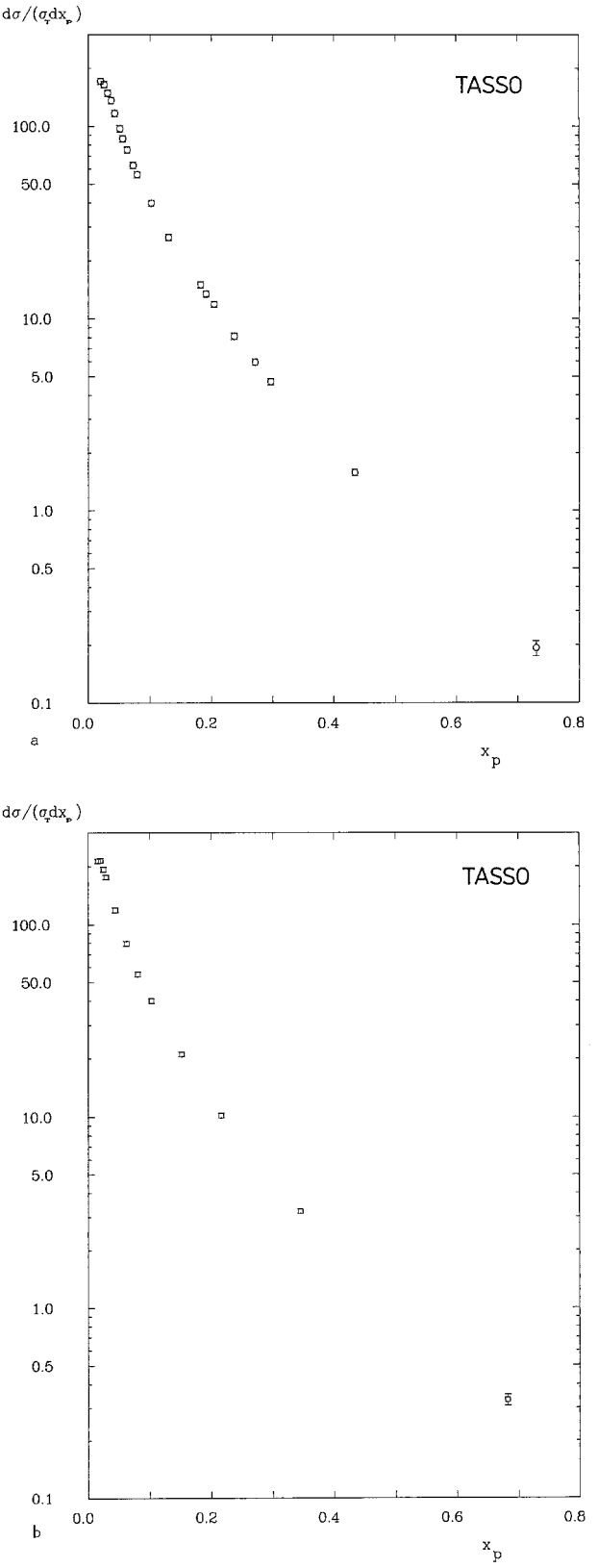

Fig. 3. Inclusive hadron cross section $d\sigma/\sigma_T dx_p$ **a** 34 GeV c.m. energy, **b** 44 GeV c.m. energy, where σ_T = total cross section, $x_p = p/p_{\text{beam}}$, p = particle momentum, p_{beam} = beam momentum. An overall 6% normalization error is not included

Table 1a. Particle fractions at 34 GeV c.m. energy

$x_p = p/p_{beam}$	$f(\pi^+ + \pi^-)$	$f(K^+ + K^-)$	$f(p+\bar{p})$
0.0171 – 0.0229	0.947 ± 0.014	0.044 ± 0.003	0.009 ± 0.005
0.0229 – 0.0286	0.922 ± 0.014	0.061 ± 0.005	0.016 ± 0.003
0.0286 – 0.0343	0.869 ± 0.015	0.108 ± 0.008	0.022 ± 0.002
0.0343 – 0.0400	0.856 ± 0.018	0.110 ± 0.013	0.034 ± 0.004
0.0400 – 0.0457	0.848 ± 0.019	0.114 ± 0.026	0.039 ± 0.009
0.0457 – 0.0571	0.822 ± 0.015	0.125 ± 0.029	0.055 ± 0.005
0.0571 – 0.0686	0.783 ± 0.056		
0.0571 – 0.0914		0.167 ± 0.036	
0.0686 – 0.0914	0.769 ± 0.048		0.073 ± 0.012
0.0914 – 0.114	0.759 ± 0.043	0.156 ± 0.070	0.085 ± 0.026
0.114 – 0.146	0.730 ± 0.040		
0.171 – 0.194	0.610 ± 0.065	0.266 ± 0.045	0.102 ± 0.032
0.194 – 0.217	0.649 ± 0.057		
0.217 – 0.263	0.616 ± 0.043	0.294 ± 0.046	0.094 ± 0.037
0.263 – 0.343	0.607 ± 0.039		
0.343 – 0.571	0.579 ± 0.038		
0.571 – 0.971	0.584 ± 0.099	0.256 ± 0.113	0.160 ± 0.081

Table 1b. Particle fractions at 44 GeV c.m. energy

$x_p = p/p_{beam}$	$f(\pi^+ + \pi^-)$	$f(K^+ + K^-)$	$f(p+\bar{p})$
0.0136 – 0.0182	0.948 ± 0.014	0.041 ± 0.006	0.011 ± 0.005
0.0182 – 0.0227	0.878 ± 0.036	0.092 ± 0.025	0.031 ± 0.006
0.0227 – 0.0273	0.860 ± 0.020	0.110 ± 0.014	0.030 ± 0.006
0.0273 – 0.0318	0.816 ± 0.028	0.133 ± 0.018	0.050 ± 0.006
0.0364 – 0.0545	0.815 ± 0.095		
0.0545 – 0.0727	0.713 ± 0.076		
0.0727 – 0.0909	0.615 ± 0.092		
0.0909 – 0.118	0.635 ± 0.098		
0.136 – 0.173	0.610 ± 0.093		
0.173 – 0.273	0.629 ± 0.047		
0.273 – 0.455	0.645 ± 0.069		
0.455 – 1.0	0.588 ± 0.126		

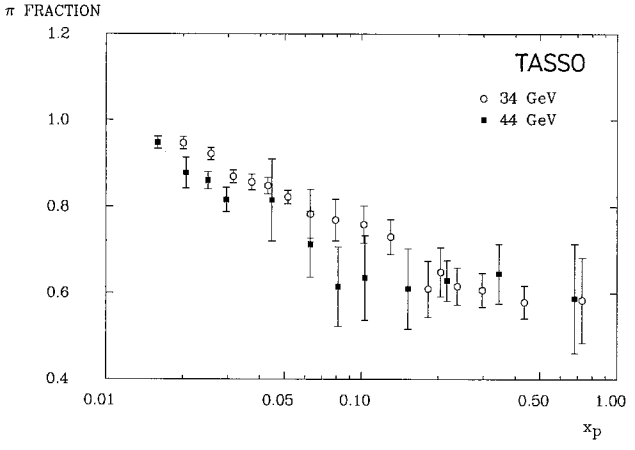

Fig. 4. Charged pion fractions $f(\pi^+ + \pi^-)$ at 34 GeV and 44 GeV c.m. energy

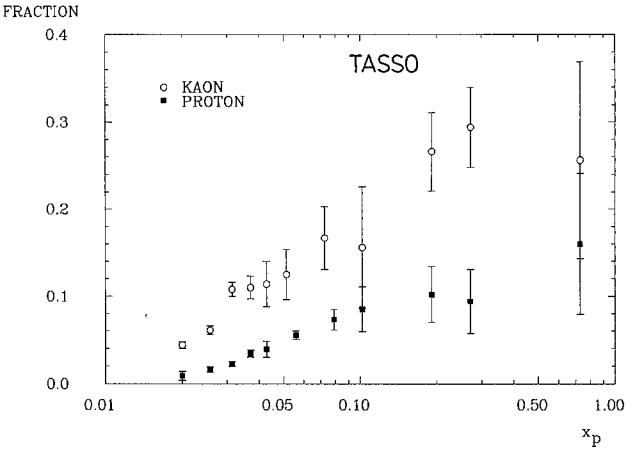

Fig. 5. Charged kaon fractions $f(K^+ + K^-)$ and proton/antiproton $f(p+\bar{p})$ at 34 GeV c.m. energy

the particle fractions. These data are shown in Tables 2a, b. The above mentioned overal 6% normalization error is not included. Statistical and systematic errors have been added in quadrature. Figure 6a, b shows the inclusive pion, kaon and proton plus antiproton cross sections at 34 GeV c.m. energy. The phase space invariant cross sections have been fitted to the form

$$\frac{E}{4\pi p^2} \cdot \frac{1}{\sigma_T} \cdot \frac{d\sigma}{dp} = \sum_{i=1}^{3} a_i \exp(-b_i E),$$

where E is the particle energy.

The results of these fits are also shown. They are used to extrapolate and interpolate at the unmeasured momenta and to estimate total particle yields.

Figure 6c, d shows the inclusive charged pion spectra at 34 GeV and 44 GeV c.m. energy for comparison. The data show deviations from scaling for small values of $x_p < 0.03$ (see also [12]).

Figure 7 shows the inclusive charged and neutral pion distribution at 44 GeV c.m. energy. To allow an easy comparison, we have plotted $\sigma(\pi^+ + \pi^-)/2$, showing that the π^0 cross section agrees with the π^+ or the π^- cross section within the errors. The differential π^0 cross section is listed in Table 3.

Our results have improved statistics and treatment of systematic effects and supersede our earlier results [3] at 34 GeV. However, new and old results agree within errors except for the charged kaon fractions between 0.4 and 1.0 GeV/c ($0.024 < x_p < 0.059$), where the new values are somewhat lower. Our results can also be compared with those of other groups working at 29 GeV c.m. energy [5]. There is good agreement (see Fig. 8a, d) except for the charged kaon fractions in the above mentioned x_p interval, where our values are higher.

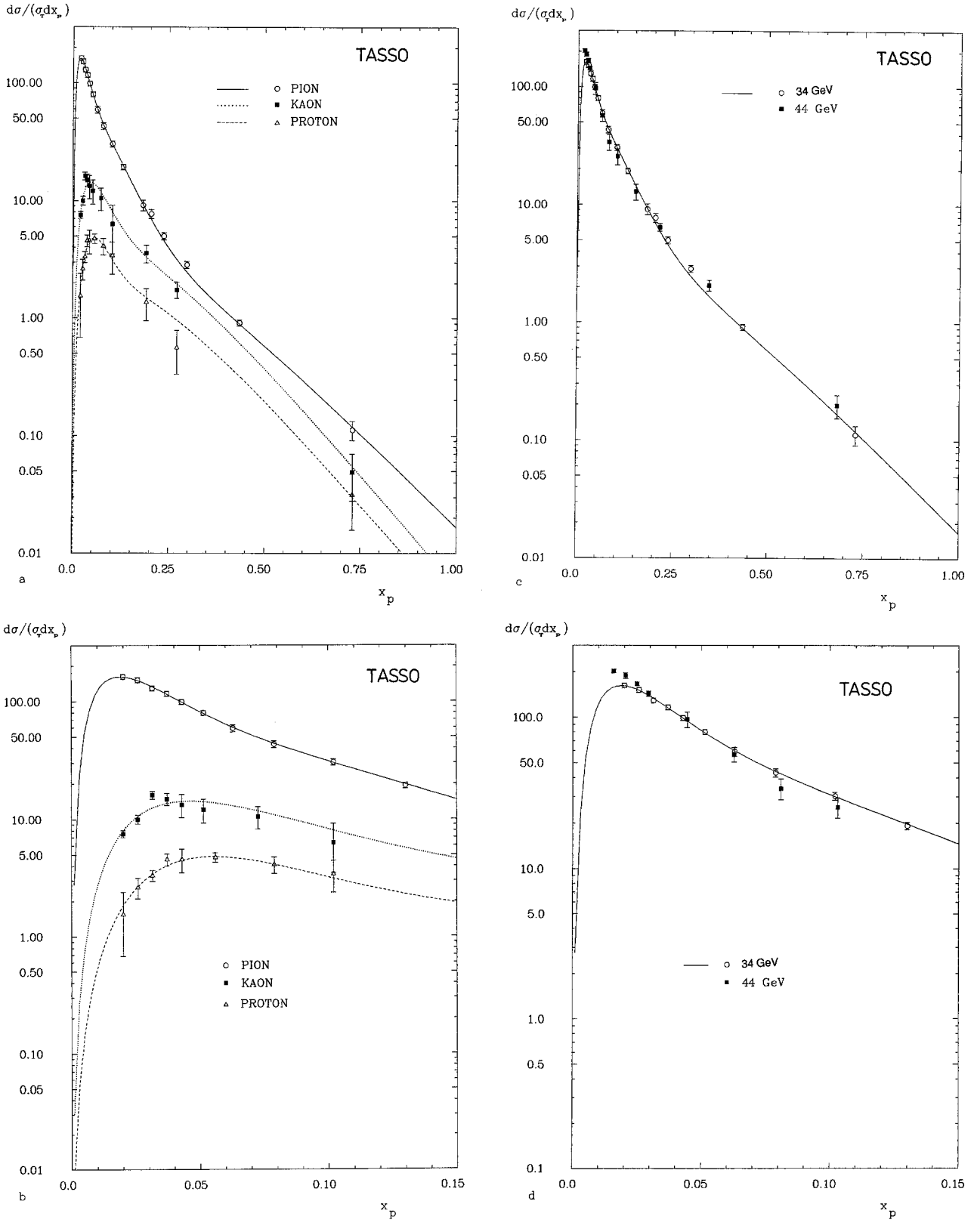

Fig. 6. **a** Differential cross sections for charged pions, charged kaons and protons plus antiprotons at 34 GeV c.m. energy $d\sigma/\sigma_T dx_p$, where σ_T = total cross section, $x_p = p/p_{\text{beam}} = 2p/\sqrt{s}$. Statistical and systematic errors have been added in quadrature, an overall 6% normalization error is not included. **b** Same as **a**, with expanded scale. **c** Charged pion cross section at 34 GeV and 44 GeV c.m. energy. **d** Same as **c**, with expanded scale

Table 2a. Inclusive cross sections at 34 GeV c.m. energy

$x_p = p/p_{beam}$	$\langle x_p \rangle$	$\frac{d\sigma(\pi^+ + \pi^-)}{\sigma_T dx_p}$	$\frac{d\sigma(K^+ + K^-)}{\sigma_T dx_p}$	$\frac{d\sigma(p+\bar{p})}{\sigma_T dx_p}$
0.0171 – 0.0229	0.020	162 ±3	7.5 ±0.5	1.54 ±0.86
0.0229 – 0.0286	0.0257	151 ±3	10.0 ±0.9	2.63 ±0.53
0.0286 – 0.0343	0.0314	129 ±3	16.1 ±1.2	3.33 ±0.35
0.0343 – 0.0400	0.0371	116 ±3	14.9 ±1.7	4.55 ±0.53
0.0400 – 0.0457	0.0429	98.9 ±2.5	13.3 ±3.0	4.55 ±1.05
0.0457 – 0.0571	0.0514	79.8 ±1.6	12.1 ±2.8	
0.0571 – 0.0686	0.0629	59.1 ±4.2		
0.0457 – 0.0686	0.056			4.74 ±0.44
0.0571 – 0.0914	0.0726		10.5 ±2.3	
0.0686 – 0.0914	0.0789	43.1 ±2.8		4.10 ±0.67
0.0914 – 0.114	0.102	30.3 ±1.7	6.3 ±2.8	3.4 ±1.03
0.114 – 0.146	0.130	19.3 ±1.1		
0.171 – 0.194	0.182	9.1 ±1.0		
0.194 – 0.217	0.204	7.7 ±0.7		
0.171 – 0.217	0.191		3.57 ±0.61	1.37 ±0.42
0.217 – 0.263	0.237	5.0 ±04		
0.263 – 0.343	0.297	2.85 ±0.19		
0.217 – 0.343	0.271		1.75 ±0.28	0.56 ±0.23
0.343 – 0.571	0.434	0.91 ±0.052		
0.571 – 0.971	0.73	0.11 ±0.02	0.05 ±0.02	0.032 ±0.016

Table 2b. Inclusive cross sections at 44 GeV c.m. energy

$x_p = p/p_{beam}$	$\langle x_p \rangle$	$\frac{d\sigma(\pi^+ + \pi^-)}{\sigma_T dx_p}$	$\frac{d\sigma(K^+ + K^-)}{\sigma_T dx_p}$	$\frac{d\sigma(p+\bar{p})}{\sigma_T dx_p}$
0.0136 – 0.0182	0.0159	202 ±4	8.8 ±1.2	2.4 ±1.1
0.0182 – 0.0227	0.0205	188 ±8	19.8 ±5.3	6.6 ±1.3
0.0227 – 0.0273	0.0250	166 ±4	21.3 ±2.6	5.7 ±1.2
0.0273 – 0.0318	0.0295	143 ±6	23.2 ±3.1	8.8 ±1.1
0.0364 – 0.0545	0.0445	96.8 ±11.4		
0.0545 – 0.0727	0.0627	56.5 ± 6.2		
0.0727 – 0.0909	0.0809	33.9 ± 5.1		
0.0909 – 0.118	0.103	25.5 ± 4.0		
0.136 – 0.173	0.152	12.9 ± 2.0		
0.173 – 0.273	0.216	6.4 ± 0.5		
0.273 – 0.455	0.345	2.1 ± 0.2		
0.455 – 1.0	0.682	0.20 ± 0.04		

Table 3. Inclusive π^0 cross section at 44 GeV c.m. energy

$x_p = p/p_{beam}$	$\langle x_p \rangle$	$\frac{d\sigma}{\sigma_T dx_p}$ ± stat. ± syst.
0.0455 – 0.0682	0.0555	39.2 ±8.1 ±8.1
0.0682 – 0.0909	0.0782	18.0 ±5.5 ±3.5
0.0909 – 0.136	0.110	11.1 ±2.1 ±2.1
0.136 – 0.182	0.156	7.2 ±1.3 ±1.3
0.182 – 0.273	0.219	2.64 ±0.57 ±0.68
0.273 – 0.545	0.391	0.57 ±0.11 ±0.13
0.545 – 1.00	0.705	0.040 ±0.015 ±0.011

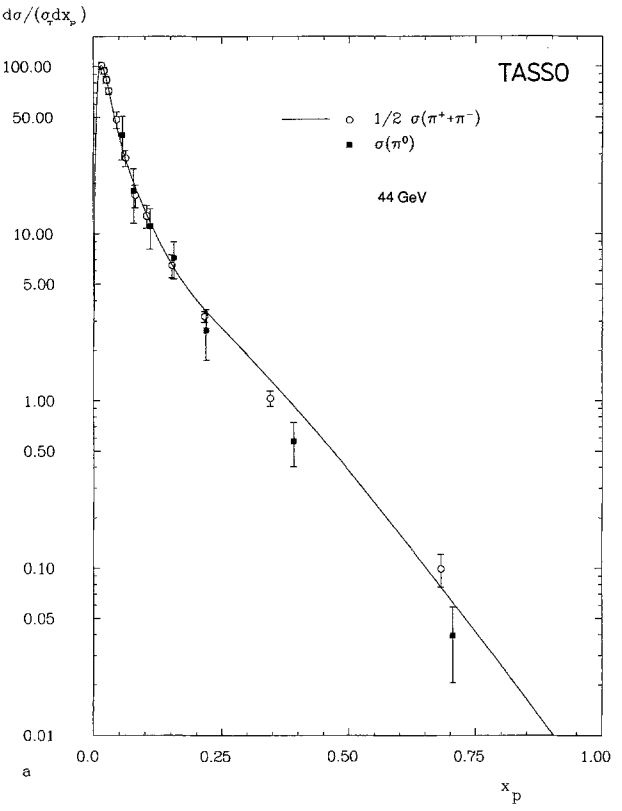

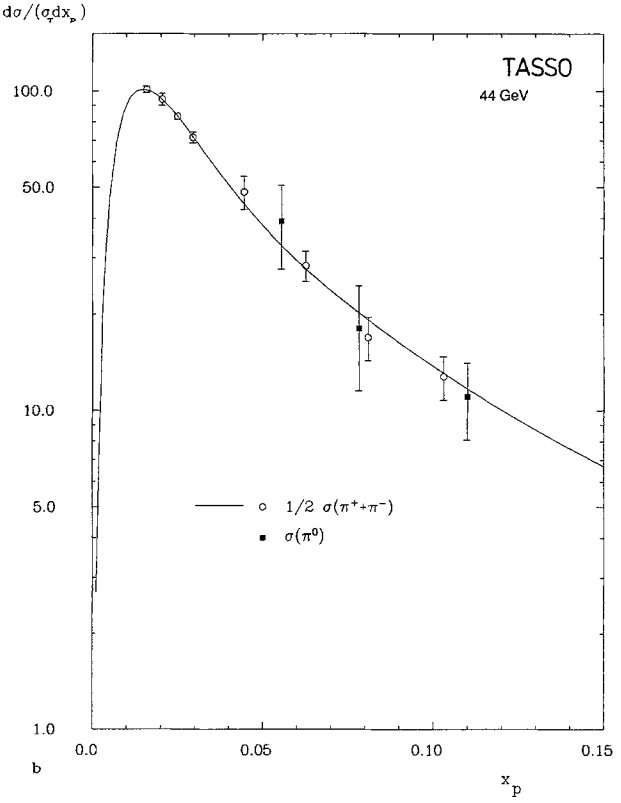

Fig. 7a, b. Differential cross sections for charged and neutral pions at 44 GeV c.m. energy: $d\sigma(\pi^0)/\sigma_T dx_p$ and $1/2 d\sigma(\pi^+ + \pi^-)/\sigma_T dx_p$, $x_p = p/p_{beam} = 2p/\sqrt{s}$. Statistical and systematic errors have been added in quadrature

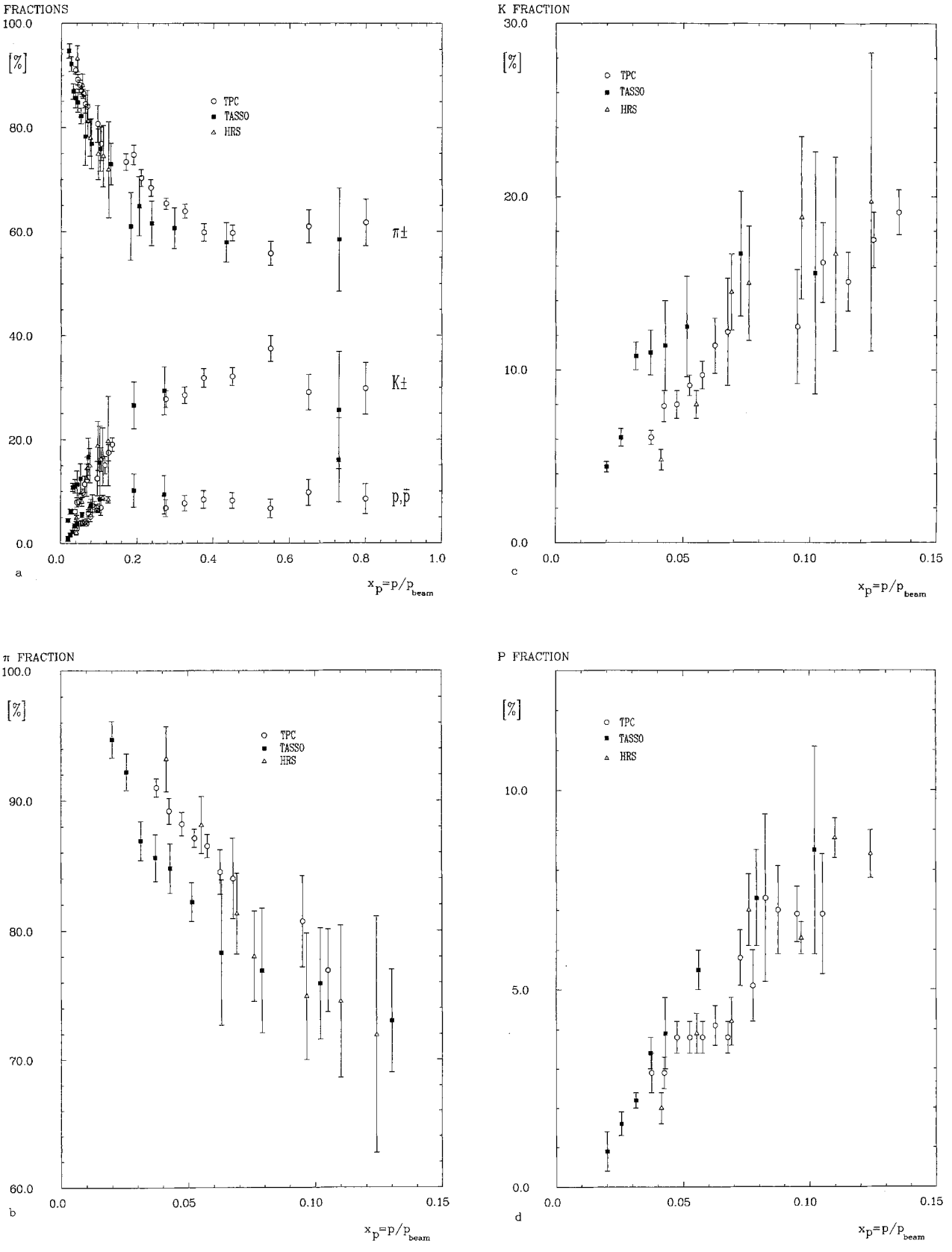

Fig. 8a–d. Comparison of the particle fractions for charged pions, charged kaons and protons/antiprotons from the TPC and HRS collaborations and this work; **a** all, **b** pions, **c** kaons, **d** protons/antiprotons

The inclusive charged hadron spectra at 34 GeV c.m. energy can be integrated to give average multiplicities of charged pions, kaons and protons plus antiprotons. The calculation requires an extrapolation to small momenta.

The result at 34 GeV c.m. energy is:

$$\langle n(\pi^+ + \pi^-)\rangle = 10.9 \pm 0.5$$
$$\langle n(K^+ + K^-)\rangle = 1.76 \pm 0.20$$
$$\langle n(p + \bar{p})\rangle = 0.67 \pm 0.06.$$

At 44 GeV c.m. energy we obtain,

$$\langle n(\pi^+ + \pi^-)\rangle = 11.1 \pm 0.5$$
$$\langle n(\pi^0)\rangle = 5.4 \pm 1.0.$$

The π^0 multiplicity has been obtained by assuming that the π^0 differential cross section is proportional to the charged pion cross section for momenta $p < 1$ GeV/c, where the π^0 cross section has not been measured (about 50% of the cross section).

This assumption is supported by the fact, that at 34 GeV c.m. energy the π^0 cross section below 1 GeV/c measured by the JADE collaboration [6] agrees with half of the charged pion cross section as measured by us.

The average π^0 multiplicity at 44 GeV can be compared with our results at 34.6 GeV [4], where we obtained $\langle n(\pi^0)\rangle = 5.8 \pm 0.9$. It is also interesting to compare the average $K^+ + K^-$ multiplicity at 34 GeV with the value obtained by us for the K^0-multiplicity $\langle n(K^0 + \bar{K}^0)\rangle = 1.48 \pm 0.05$ at the same c.m. energy [13].

Acknowledgements. We gratefully acknowledge the support of the DESY directorate, the PETRA machine group and the staff of the DESY computer center. Those of us from outside DESY wish to thank the DESY directorate for the hospitality extended to us.

References

1. TASSO Coll. R. Brandelik et al.: Phys. Lett. 94 B (1980) 444
2. TASSO Coll. R. Brandelik et al.: Phys. Lett.108 B (1982) 71
3. TASSO Coll. M. Althoff et al.: Z. Phys. C – Particles and Fields 17 (1983) 5
4. TASSO Coll. W. Braunschweig et al.: Z. Phys. C – Particles and Fields 33 (1986) 13
5. TPC/Two-Gamma Coll. H. Aihara et al.: Phys. Rev. Lett. 52 (1984) 577; Mark II Col. H. Schellmann et al.: Phys. Rev. D 31 (1985) 3013; HRS Coll. M. Derrick et al.: Phys. Rev. D 35 (1987) 2639; TPC/Two-Gamma Coll. H. Aihara et al.: LBL-24896 (1988); Phys. Rev. Lett. 61 (1988) 1263
6. TPC/Two-Gamma Coll. H. Aihara et al.: Z. Phys. C – Particles and Fields 27 (1985) 187; JADE Coll. W. Bartel et al.: Z. Phys. C – Particles and Fields 28 (1985) 343; CELLO Coll. H.-J. Behrend et al.: Z. Phys. C – Particles and Fields 14 (1982) 189; H.-J. Behrend et al.: Z. Phys. C – Particles and Fields 20 (1983) 207
7. TASSO Coll. R. Brandelik et al.: Phys. Lett. 113 B (1982) 9
8. K.W. Bell et al.: Nucl. Instrum. Methods 179 (1981) 27
9. H.L. Krasemann: Ph.D. Thesis Hamburg 1985
10. P. Rehders: Diploma Thesis, Hamburg 1987
11. TASSO Coll. M. Althoff et al.: Z. Phys. C – Particles and Fields 22 (1984) 307
12. TASSO Coll. R. Brandelik et al.: Phys. Lett. 114 B (1982) 65
13. TASSO Coll. M. Althoff et al.: Z. Phys. C – Particles and Fields 27 (1985) 27